

Proposal for ultrafast switching of ferroelectrics using mid-infrared pulses

Alaska Subedi

*Max Planck Institute for the Structure and Dynamics of Matter,
Luruper Chaussee 149, 22761 Hamburg, Germany*

(Dated: October 8, 2018)

I propose a method for ultrafast switching of ferroelectric polarization using mid-infrared pulses. This involves selectively exciting the highest frequency A_1 phonon mode of a ferroelectric material with an intense mid-infrared pulse. Large amplitude oscillations of this mode provides a unidirectional force to the lattice such that it displaces along the lowest frequency A_1 phonon mode coordinate because of a nonlinear coupling of the type $gQ_P Q_{IR}^2$ between the two modes. First principles calculations show that this coupling is large in perovskite transition-metal oxide ferroelectrics, and the sign of the coupling is such that the lattice displaces in the switching direction. Furthermore, I find that the lowest frequency A_1 mode has a large Q_P^3 order anharmonicity, which causes a discontinuous switch of electric polarization as the pump amplitude is continuously increased.

PACS numbers: 77.80.Fm, 78.20.Bh, 63.20.Ry, 78.47.J-

I. INTRODUCTION

Ultrafast switching of polarization in ferroelectrics is of great interest for potential application in non-volatile memory devices. FLASH memories, which at present are the most commonly used non-volatile memory devices, have an operating speed of milliseconds. Because of their slow speed, they are not considered as candidates for future memory applications¹. Other emerging non-volatile memory technologies that utilize phase or resistance change have write and erase times of nanoseconds. Therefore, development of a switching mechanism at sub-picosecond timescales has the potential to revolutionize the field.

Non-destructive readout of the electric polarization at sub-picosecond timescales has recently been demonstrated by analyzing the THz pulse waveforms radiated after illumination of a ferroelectric sample by femtosecond laser pulses at optical wavelengths^{2,3}. This makes ferroelectric materials an exciting prospect for memory applications if switching can be achieved at similarly ultrashort timescales.

Ferroelectric materials exhibit remnant polarization even at zero external electric field because the cations and anions in these materials are asymmetrically displaced in the equilibrium structure. To switch the polarization, the relative displacement between the cations and anions need to be reversed. This can be achieved by applying a (quasi-)static electric field because such an electric field imparts a unidirectional force to the cations and anions. An arbitrary light pulse, whose oscillating electric field integrates to zero by definition, imparts a zero total force to the electric dipole present in the material. Therefore, an ultrashort light pulse cannot in general be used to switch the polarization of a ferroelectric material. Nevertheless, there have been several proposals for switching the polarization of ferroelectric materials using ultrashort light pulses by controlling their soft phonon modes^{4,5}.

In this paper, I propose a method for using mid-infrared pulses that are resonant with the highest fre-

quency infrared-active phonon mode of a perovskite transition-metal oxide ferroelectric to switch its polarization. This involves controlling the dynamical degrees of freedom of the lattice and requires four main ingredients. First, I notice that there always exists a low frequency fully symmetric A_1 phonon mode in the ferroelectric phase that involves the motion of the cations and anions of the material in a way that changes the electric polarization. Second, I find that this phonon mode couples to the highest frequency infrared-active A_1 phonon mode of the material with a large $gQ_P Q_{IR}^2$ coupling, where g is the coupling constant and Q_P and Q_{IR} are the normal mode coordinates of the lowest frequency and highest frequency A_1 normal mode coordinates, respectively. Third, I find from first principles calculations that the sign of the coupling is such that the excitation of the highest frequency A_1 mode provides a displacive force along the Q_P normal mode coordinate in the direction that switches the polarization. Fourth, I find that the Q_P mode has a strong Q_P^3 order anharmonicity, which facilitates an abrupt switch of electric polarization as the Q_{IR} amplitude is continuously increased. Coherent displacement along Raman mode coordinates utilizing nonlinear phonon couplings by resonantly exciting the highest frequency infrared mode of various centrosymmetric oxides has previously been demonstrated⁶⁻⁹. Therefore, the method proposed here to switch ferroelectric polarization at ultrafast timescales using mid-infrared pulses is experimentally feasible.

II. COMPUTATIONAL DETAILS

I illustrate the proposed mechanism for the case of PbTiO_3 . The phonon frequencies and eigenvectors and the nonlinear couplings between two phonon modes were obtained using density functional theory calculations with plane-wave basis sets and projector augmented wave pseudopotentials^{10,11} as implemented in the VASP software package¹². The interatomic force constants were

calculated using the frozen-phonon method¹³, and the PHONOPY software package was used to calculate the phonon frequencies and eigenvectors¹⁴. Total energy calculations were then performed as a function of the lowest frequency Q_P and high-frequency Q_{IR} coordinates to obtain energy surfaces. The nonlinear couplings between the two modes were obtained by fitting the calculated energy surface to the polynomial shown in Eq. 1.

I used the experimental values of $a = 3.9039$ and $c = 4.1348$ Å for the tetragonal lattice parameters but relaxed the atomic positions. The calculations were performed within the local density approximation. A cut-off of 600 eV was used for the plane-wave basis set expansion, and an $8 \times 8 \times 8$ k -point grid was used in the Brillouin zone integration.

III. RESULTS AND DISCUSSIONS

The ferroelectric phase of PbTiO_3 exists in the $P4mm$ structure with one formula unit per unit cell. This gives rise to 12 zone-center optical normal modes with the decomposition $\Gamma_{\text{optic}} = 3A_1 + B_1 + 4E$. The A_1 and E modes are both Raman and infrared active, whereas the B_1 is only Raman active. The calculated zone center phonon frequencies and their symmetries are given in Table I. I find that the coupling between the lowest frequency E and the highest frequency A_1 mode is weak. Therefore, I focus on the coupled dynamics of the lowest and highest frequency A_1 modes.

The atomic displacement pattern of the lowest frequency A_1 mode (denoted by Q_P) is shown in Fig. 1(a) with z axis chosen as the polarization axis. A finite magnitude of this mode involves the motion of Pb^{2+} and O^{2-} ions along the z axis in the opposite direction, and a displacement of the lattice along the coordinate of this mode modifies the electric polarization of the material. In the convention used in this paper, a large negative value of this normal mode coordinate would reverse the polarization. The arrows in Fig. 1(a) indicate the movements of ions for such a negative value of Q_P . One can see that such a movement reverses the relative dis-

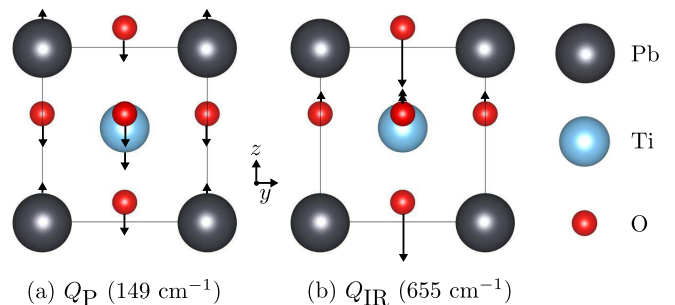


FIG. 1: (Color online) Displacement patterns of the (a) lowest frequency (149 cm^{-1}) Q_P and (b) highest frequency (655 cm^{-1}) Q_{IR} modes of the ferroelectric phase of PbTiO_3 . Both modes belong to the A_1 irreducible representation.

placement between the Pb^{2+} and O^{2-} ions. However, it should be noted that a displacement along this mode does not bring the structure to the symmetrically equivalent ground state with opposite polarization because the eigenvector of this mode is not in general equal to the eigenvector of the unstable infrared mode of the paraelectric phase that is responsible for the ferroelectric instability. A further relaxation of the lattice, in addition to the large negative value of the Q_P coordinate that reverses the polarization, would take the structure to the symmetrically equivalent switched ground state. I confirmed this by starting with a structure that was displaced by a value of $-8 \text{ \AA} \sqrt{\text{amu}}$ along the Q_P coordinate and relaxing the atomic positions by minimizing the forces. I found that the structure indeed relaxes to the symmetrically equivalent switched phase rather than going back to the initial ferroelectric equilibrium state that was used as a starting point to displace along the Q_P coordinate.

Therefore, a coherent displacement of the lattice along this low frequency Q_P phonon mode coordinate is a viable route for ultrafast ferroelectric switching. In fact, Qi *et al.* have proposed a method for switching the polarization by driving large amplitude oscillations of this phonon mode using multiple THz pulses with an asymmetric electric field profile⁵.

Here I propose a method of switching the polarization using a light pulse that does not directly drive the low frequency Q_P mode. Instead, this involves exciting the high frequency Q_{IR} infrared mode of the material (shown in Fig. 1(b)) by an intense mid-infrared pulse that in turn provides a displacive force along the Q_P coordinate in the switching direction due to a nonlinear coupling of the type $gQ_P Q_{IR}^2$ between the two modes. Furthermore, the presence of a large Q_P^3 order anharmonicity causes a sudden increase in the displacement along the Q_P coordinate as the Q_{IR} amplitude is continuously increased, and this causes an abrupt reversal of the electric polarization without the magnitude of the polarization going to zero.

I calculated the total energy as a function of the lowest frequency Q_P and highest frequency Q_{IR} infrared mode coordinates from first principles using density functional theory calculations. The calculated energy surface of fer-

TABLE I: The zone-center phonon frequencies and their irreducible representation and optical activity of ferroelectric PbTiO_3 .

frequency (cm^{-1})	irrep	optical activity
80	E	IR + Raman
149	A_1 (Q_P)	IR + Raman
187	E	IR + Raman
273	E	IR + Raman
290	B_1	Raman
356	A_1	IR + Raman
491	E	IR + Raman
655	A_1 (Q_{IR})	IR + Raman

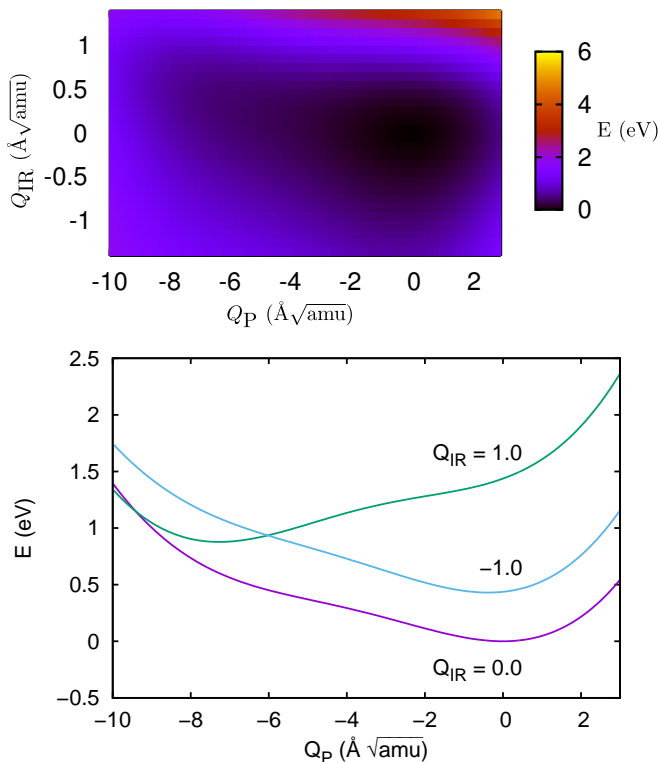


FIG. 2: (Color online) Total energy as a function of the Q_P and Q_{IR} normal mode coordinates of the ferroelectric PbTiO_3 . Top: energy surface. Bottom: few energy curves that illustrate the behavior of the Q_P mode as a function of Q_{IR} mode.

roelectric PbTiO_3 is shown in Fig. 2, and it fits the following expression:

$$\begin{aligned}
 V(Q_P, Q_{IR}) = & \frac{1}{2}\Omega_P^2 Q_P^2 + \frac{1}{2}\Omega_{IR}^2 Q_{IR}^2 + \frac{1}{3}a_3 Q_P^3 \\
 & + \frac{1}{4}a_4 Q_P^4 + \frac{1}{3}b_3 Q_{IR}^3 + \frac{1}{4}b_4 Q_{IR}^4 \\
 & + g Q_P Q_{IR}^2 + h Q_P^2 Q_{IR} + i Q_P^3 Q_{IR} \\
 & + j Q_P Q_{IR}^3 + k Q_P^2 Q_{IR}^3 + l Q_P Q_{IR}^4. \quad (1)
 \end{aligned}$$

A fit of the above expression to the calculated energy surface determines *ab initio* the nonlinear couplings between the two modes up to all significant orders of the two phonon coordinates. The values of the coefficients of the coupling terms obtained from such a fit are given in Table II. The calculated energy surface exhibits complex features, and this is due to the presence of both even and odd order nonlinearities. However, there are some salient features. When $Q_{IR} = 0$, the energy curve of the Q_P mode has one minimum at zero, as one would expect for a stable ground-state structure. The energy increases rapidly for positive values of Q_P , but the increase is less rapid for negative values of Q_P . In fact, for negative values of Q_P , the slope of the energy curve has a minimum near $-5 \text{ \AA}\sqrt{\text{amu}}$, where the energy curve is shallow and the restoring force is small, before it shows

an upturn around $-8 \text{ \AA}\sqrt{\text{amu}}$. This asymmetric nature of the energy curve of the Q_P mode is due to the presence of a large $a_3 Q_P^3$ term in the polynomial expression of the energy surface. The physical reason for the asymmetric nature of the Q_P energy curve is the presence of a state with reversed polarization near a Q_P value of $-8 \text{ \AA}\sqrt{\text{amu}}$ that is symmetrically equivalent to the ferroelectric state at a Q_P value of zero.

TABLE II: The anharmonic terms and nonlinear couplings of the Q_P and Q_{IR} modes of ferroelectric PbTiO_3 determined from a fit to the energy surface calculated from first principles.

coefficient	value
a_3 (meV/amu ^{3/2} /Å ³)	21.80
a_4 (meV/amu ² /Å ⁴)	1.89
b_3 (meV/amu ^{3/2} /Å ³)	1567.65
b_4 (meV/amu ² /Å ⁴)	631.80
g (meV/amu ^{3/2} /Å ³)	70.32
h (meV/amu ^{3/2} /Å ³)	-12.40
i (meV/amu ² /Å ⁴)	-0.79
j (meV/amu ² /Å ⁴)	52.14
k (meV/amu ^{5/2} /Å ⁵)	2.29
l (meV/amu ^{5/2} /Å ⁵)	7.61

The energy surface is also asymmetric in the Q_{IR} coordinate because of the presence of odd order terms. The presence of both even and odd order terms is consistent with the fact that this high frequency mode also has the A_1 representation that does not break any crystal symmetry and is both infrared and Raman active. Although the energy surface is asymmetric in the Q_{IR} coordinate, both positive and negative Q_{IR} displacements move the minimum of the Q_P coordinate towards the negative direction. A negative value of Q_{IR} displaces the lattice towards the negative Q_P direction by a modest amount. However, a positive value of Q_{IR} does not continuously shift the energy curve near the negative Q_P direction. It raises the energy curve near $Q_P \approx 0$ and creates an energy minimum at a large negative value of the Q_P coordinate such that a state with reversed polarization is energetically favored. This abrupt shift of the minimum of the Q_P mode is due to the presence of a large $a_3 Q_P^3$ term.

If the oscillations along the Q_{IR} coordinate are integrated out, the average potential experienced by the lattice has a minimum at a negative value of the Q_P coordinate with the magnitude of the displacement along Q_P coordinate depending on the integration cut-off (i.e., the amplitude of the Q_{IR} oscillations). This is because the coupling constant g of the term $Q_P Q_{IR}^2$ has the largest magnitude, and it implies that the lattice will experience a large unidirectional force $-\partial V/\partial Q_P = -g Q_{IR}^2$ along the Q_P coordinate when the Q_{IR} mode is being driven. Furthermore, a large $a_3 Q_P^3$ term ensures that the displacement of the lattice along the Q_P coordinate abruptly increases as the Q_{IR} amplitude is continuously

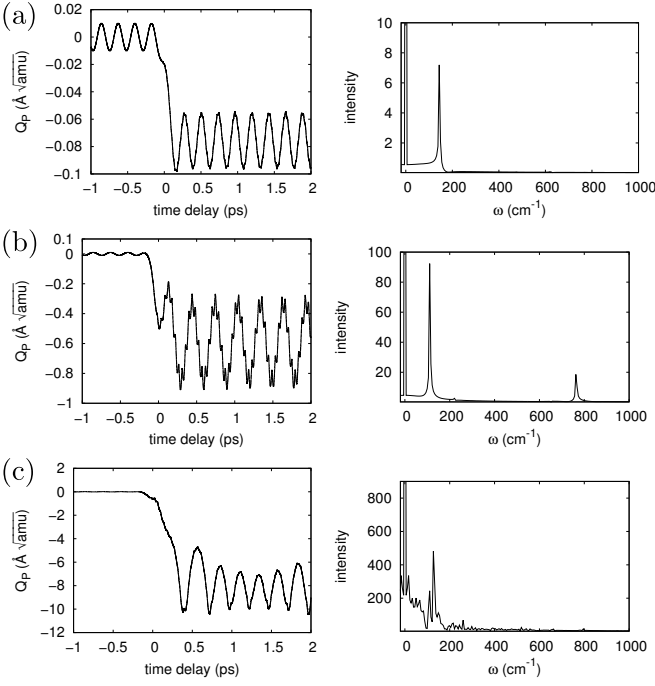


FIG. 3: Dynamics of the Q_P mode for three different pump amplitudes. Left panels: Displacements along Q_P coordinate as function of time delay. Right panels: Fourier transform of the positive time delay oscillations.

increased, which causes the electric polarization to switch discontinuously.

We can achieve a better understanding of the dynamics of the lattice when the Q_{IR} mode is pumped externally by a mid-infrared pulse by treating the Q_P and Q_{IR} modes as classical oscillators and studying their coupled equations of motion. In this picture, the two oscillators experience a force deriving from the calculated energy surface, and the Q_{IR} mode is additionally driven by a term $F(t) = F \sin(\Omega t) e^{-t^2/2\sigma^2}$, where F , σ , and Ω are the amplitude, width, and frequency of the mid-infrared pulse, respectively. By treating the expression in Eq. 1 as the potential, the coupled equations motion are

$$\begin{aligned}
 \ddot{Q}_{IR} + \Omega_{IR}^2 Q_{IR} &= -b_3 Q_{IR}^2 - b_4 Q_{IR}^3 - 2g Q_P Q_{IR} \\
 &\quad - h Q_P^2 - i Q_P^3 - 3j Q_P Q_{IR}^2 \\
 &\quad - 3k Q_P^2 Q_{IR}^3 - 4l Q_P Q_{IR}^3 + F(t), \\
 \ddot{Q}_P + \Omega_P^2 Q_P &= -a_3 Q_P^2 - a_4 Q_P^3 - g Q_{IR}^2 \\
 &\quad - 2h Q_P Q_{IR} - 3i Q_P^2 Q_{IR} - j Q_{IR}^3 \\
 &\quad - 2k Q_P Q_{IR}^3 - l Q_{IR}^4. \quad (2)
 \end{aligned}$$

The results from numerical integration of the coupled equation of motions for different pump amplitudes are shown in Fig. 3. In these calculations, I have used a pump pulse with a symmetric Gaussian profile and a width of $\sigma = 250$ fs, which correspond to typical pump pulses used in mid-infrared excitations^{6,7,9}. A pump frequency of $\Omega = 1.03 \Omega_{IR}$ was used in the simulations, which is chosen to be slightly off-resonance with the frequency of the Q_{IR}

mode to demonstrate that this method is efficacious even if the pump pulse is not precisely resonant with the Q_{IR} mode.

Even for small pump amplitudes that cause a change in the Ti-apical O distances of a few percent along the Q_{IR} coordinate, the Q_P mode oscillates at a displaced position in the negative Q_P direction (see the left panel of Fig. 3(a)). This is consistent with the analysis of the $g Q_P Q_{IR}^2$ coupling presented in Refs. 6 and 8. In Ref. 8, it was shown that the Q_P mode experiences an effective force $-g Q_{IR}^2 \propto -g F^2 \Omega_{IR}^2 \sigma^6 (1 - \cos 2\Omega_{IR} t)$ when the Q_{IR} mode is pumped by an external driving term $F(t)$, and the time average of this forcing field has a rectified non-zero value. The oscillation of the Q_P mode at a rectified position is also seen in the Fourier transform of the time evolution of the Q_P mode at positive time delays as shown in the right panel of Fig. 3(a). The Fourier transform shows a peak at zero frequency that is due to the displacement of the lattice along the Q_P coordinate. In addition, there is a peak at Ω_P and a negligible presence of higher-harmonics, which shows that the dynamics of the coupled oscillators are determined by the $g Q_P Q_{IR}^2$ term, and other nonlinearities only play a marginal role at small pump amplitudes. At small pump amplitudes, the displacement along the negative direction in the Q_P coordinate is small. Therefore, although the electric polarization is reduced, the reversal of the polarization has not occurred.

It is also noteworthy that the cubic terms in the energy potential $a_3 Q_P^3$ and $b_3 Q_{IR}^3$ are large. These also impart unidirectional forces $-\partial V/\partial Q_P = -a_3 Q_P^2$ and $-\partial V/\partial Q_{IR} = -b_3 Q_{IR}^2$ to their respective coordinates when the amplitude of the oscillations are large, and the lattice will be rectified along these coordinates for the reasons described in the previous paragraph. From my first principles calculations of the energy surface, I find that the coefficients of these terms are such that the lattice is rectified along the direction that reverses the electric polarization.

As the pump amplitude is increased, the effects of the abovementioned nonlinearities start to become noticeable. The oscillations of the Q_P mode start to show higher frequency components due to the presence of various nonlinear terms. Further increase of the pump amplitude takes the dynamics to a highly nonlinear regime. In this regime, the frequency at which the Q_P mode oscillates also changes. Interestingly, there are two different mechanisms that change the effective frequency of the Q_P mode. First, a large amplitude oscillation of the Q_P mode causes a change in the effective spring constant due to the $\frac{1}{4} a_4 Q_P^4$ nonlinearity in the energy potential. In the equation of motion, this nonlinearity acts to modify the frequency of the Q_P mode with a term $-\partial V/\partial Q_P = -a_4 Q_P^3$. The effective frequency $\Omega_P^{\text{eff}} \rightarrow \Omega_P^2 (1 + a_4 Q_P^2(t)/\Omega_P^2)$ changes because the time-averaged Ω_P^{eff} has a value different from Ω_P when the Q_P amplitude is large. The rectification of the lattice along the Q_P and Q_{IR} coordinates provides the second cause

for the modification of the effective frequency. For example, the rectification along the Q_P coordinate changes the effective frequency to $\Omega_P^{\text{eff}} \rightarrow \Omega_P^2 (1 + a_3 Q_P(t)/\Omega_P^2)$ due to the $a_3 Q_P^3$ term in the energy potential. The $h Q_P^2 Q_{\text{IR}}$ term in the energy potential similarly changes the effective frequency as $\Omega_P^{\text{eff}} \rightarrow \Omega_P^2 (1 + 2h Q_{\text{IR}}(t)/\Omega_P^2)$. Fig. 3(b) shows the results of the numerical integration of the equations of motion for a pump amplitude that rectifies the lattice close to a point where the polarization switches. Near the polarization reversal, the slope of the potential for the Q_P mode is less steep, and the Q_P mode oscillates at a smaller frequency. In this regime, the pumped Q_{IR} mode is oscillating at a displaced position with an amplitude that changes the two Ti-apical O bond lengths by 0.4 and 0.7 Å. These are large amplitude oscillations, but they are comparable to the change in the Ti-apical O distance of 0.6 Å when a polarization switch occurs.

Fig. 3(c) illustrates the case where the lattice moves to a far distance in the negative direction along the Q_P coordinate, and this signals that the polarization has been switched. The pump strength used in this instance causes the Q_{IR} mode to oscillate at a displaced position with an amplitude that changes the two Ti-apical O bond lengths by 0.5 and 0.8 Å. In this regime, the oscillations about the displaced position exhibit a strong nonlinear behavior with the presence of a wide range of frequency components. Nevertheless, the frequency component that has the largest spectral weight stiffens once the displacement along Q_P coordinate advances through the point of polarization reversal, although the frequency is still smaller than Ω_P .

I find that the displacement along the Q_P coordinate shows a sudden jump when the externally pumped Q_{IR} amplitude is continuously increased. This is consistent with the behavior of the energy potential discussed above where a large $a_3 Q_P^3$ term causes an abrupt change in the position of the minimum of the Q_P mode as Q_{IR} is continuously increased. As a function of the pump amplitude, the displacement along the Q_P coordinate continuously increases from a value of zero to $\sim -1.5 \text{ \AA} \sqrt{\text{amu}}$. However, a further increase of the pump amplitude causes the Q_P mode to oscillate about a displaced position of $\sim -9.0 \text{ \AA} \sqrt{\text{amu}}$. This indicates that the electric polarization switches in an abrupt, discontinuous manner when the Q_{IR} mode is externally pumped. Such a behavior can also be gleaned from the change in the frequency of the Q_P mode as the polarization reversal happens. I find that the frequency of the Q_P mode decreases by up to 60% as it is displaced along this coordinate. But it does not soften completely to zero as the polarization switch occurs and the frequency starts to increase again.

In the study presented here, nonlinear couplings between two phonon modes and their dynamics when the higher frequency mode is externally pumped has been used to predict that ferroelectric materials can be switched using mid-infrared pulses. However, in real materials there are additional dynamical degrees of freedom,

and this has two main implications. First, scattering with other degrees of freedom will cause the phonon modes to be damped. Therefore, the rectifying force along the Q_P coordinate exists only as long as the Q_{IR} mode is being externally pumped. Second, other degrees of freedom also respond to the displacement of the lattice along the Q_P coordinate. If the pump pulse is long enough, other degrees of freedom relax relative to the switched state, and this forms an energy barrier that prevents the lattice to move back to the initial state even in the absence of the pump. A more detailed theoretical study based on molecular dynamics simulations would be required to ascertain the time it would take to form the energy barrier.

As mentioned above, I performed a full relaxation of the lattice starting from a structure that corresponds to a Q_P displacement of $-8.0 \text{ \AA} \sqrt{\text{amu}}$ and found that the lattice indeed relaxes to the symmetrically equivalent switched state. The relaxation of the whole lattice to the symmetrically equivalent state with reversed polarization provides a mechanism for repeated switching because the lattice again experiences a unidirectional force in the switching direction along the Q_P coordinate when the lattice is excited anew by mid-infrared pulse.

In addition to PbTiO_3 , I investigated the nonlinear couplings between the lowest and highest frequency A_1 modes of BaTiO_3 and LiNbO_3 . I find a large $g Q_P Q_{\text{IR}}^2$ coupling between the lowest frequency A_1 mode (Q_P) and the highest frequency A_1 mode (Q_{IR}) in these materials as well. The sign of the coupling is such that the electric polarization of these materials could also be switched by pumping the Q_{IR} mode with a mid-infrared pulse. Therefore, the method illustrated here seems applicable in general to all perovskite transition-metal oxide ferroelectrics.

IV. SUMMARY

In summary, I have illustrated that the polarization of PbTiO_3 can be switched by exciting the highest frequency infrared active A_1 phonon mode of this material with a mid-infrared pulse. A large amplitude oscillation of this mode provides a unidirectional force along the lowest frequency A_1 phonon mode coordinate due to a nonlinear coupling of the type $g Q_P Q_{\text{IR}}^2$. A displacement of the lattice along the Q_P coordinate changes the electric polarization and can bring the system near the symmetrically equivalent switched state. From my first principles calculations, I find that sign of the coupling is such that the oscillations of the Q_{IR} mode displaces the lattice along the Q_P coordinate in the switching direction. I also find that the switching occurs discontinuously because of the presence of a large $a_3 Q_P^3$ term in the energy potential, which abruptly moves the minimum of the Q_P mode as the $g Q_P Q_{\text{IR}}^2$ term gets continuously larger.

In addition to PbTiO_3 , I find the presence of a similar $g Q_P Q_{\text{IR}}^2$ coupling and a large $a_3 Q_P^3$ anharmonicity in BaTiO_3 and LiNbO_3 , and this type of nonlinear coupling

seems to be universally present in perovskite transition-metal oxide ferroelectrics. Therefore, a selective excitation of the Q_{IR} mode using a mid-infrared pulse can be a general method to switch the polarization of perovskite transition-metal oxide ferroelectrics.

V. ACKNOWLEDGMENTS

I am indebted to Yannis Laplace for valuable discussions. I also acknowledge Antoine Georges, Roman

Mankowsky, Srivats Rajasekaran, and Andrea Cavalleri for helpful comments and discussions.

-
- ¹ D. S. Jeong, R. Thomas, R. S. Katiyar, J. F. Scott, H. Kohlstedt, A. Petraru, and C. S. Hwang, *Rep. Prog. Phys.* **75**, 076502 (2012).
- ² K. Takahashi, N. Kida, and M. Tonouchi, *Phys. Rev. Lett.* **96**, 117402 (2006).
- ³ D. Talbayev, S. Lee, S.-W. Cheong, and A. J. Taylor, *Appl. Phys. Lett.* **93**, 212906 (2008).
- ⁴ S. Fahy and R. Merlin, *Phys. Rev. Lett.* **73**, 1122 (1994).
- ⁵ T. Qi, Y.-H. Shin, K.-L. Yeh, K. A. Nelson, and A.M. Rappe, *Phys. Rev. Lett.* **102**, 247603 (2009).
- ⁶ M. Först, C. Manzoni, S. Kaiser, Y. Tomioka, Y. Tokura, R. Merlin, and A. Cavalleri, *Nature Phys.* **7**, 854 (2011).
- ⁷ M. Först, R. Mankowsky, H. Bromberger, D. M. Fritz, H. Lemke, D. Zhu, M. Chollet, Y. Tomioka, Y. Tokura, R. Merlin, J. P. Hill, S. L. Johnson, and A. Cavalleri, *Solid State Commun.* **169**, 24 (2013).
- ⁸ A. Subedi, A. Cavalleri, and A. Georges, *Phys. Rev. B* **89**, 220301 (2014).
- ⁹ R. Mankowsky, A. Subedi, M. Först, S. O. Mariager, M. Chollet, H. T. Lemke, J. S. Robinson, J. M. Glowia, M. P. Minitti, A. Frano *et al.*, *Nature* **516**, 71 (2014).
- ¹⁰ P. E. Blöchl, *Phys. Rev. B* **50**, 17953 (1994).
- ¹¹ G. Kresse and D. Joubert, *Phys. Rev. B* **59**, 1758 (1999).
- ¹² G. Kresse and J. Furthmüller, *Phys. Rev. B* **54**, 11169 (1996).
- ¹³ K. Parlinski, Z.-Q. Li, and Y. Kawazoe, *Phys. Rev. Lett.* **78**, 4063 (1997).
- ¹⁴ A. Togo, F. Oba, and I. Tanaka, *Phys. Rev. B* **78**, 134106 (2008).